Journal of Alloys and Compounds 509 (2011) 5996–6003

Contents lists available at ScienceDirect

Journal of Alloys and Compounds

journal homepage: www.elsevier.com/locate/jallcom

A thermodynamic modeling of the C–Cr–Ta ternary system

Chunsheng Sha[a,b], Mengjie Bu[a,b], Honghui Xu[a,b], Yong Du[a,b,*], Shequan Wang[c], Guanghua Wen[c]

[a] Research Institute of Powder Metallurgy, Central South University, Changsha, Hunan 410083, PR China
[b] Science Center for Phase Diagram & Materials Design and Manufacture, Central South University, Changsha, Hunan 410083, PR China
[c] China Zhuzhou Cemented Carbide Cutting Tools Co., LTD, Zhuzhou, Hunan 412007, PR China

ARTICLE INFO

Article history:
Received 1 October 2010
Received in revised form 20 January 2011
Accepted 28 January 2011
Available online 4 February 2011

Keywords:
C–Cr–Ta ternary system
Phase diagrams
Thermodynamic modeling

ABSTRACT

The experimental phase diagram data of the C–Cr–Ta ternary system available in the literature were critically reviewed. A thermodynamic modeling of the ternary system was then conducted by taking into account the literature data including the isothermal sections and invariant reactions. A set of self-consistent thermodynamic parameters for the Gibbs energies of individual phases in the C–Cr–Ta system was obtained by using the CALPHAD approach. Comprehensive comparisons between the calculated and measured phase diagrams show that all the reliable experimental information is satisfactorily accounted for by the present thermodynamic description.

© 2011 Elsevier B.V. All rights reserved.

1. Introduction

The alloys based on quasi-binary metal-carbide eutectics, which could be considered as in situ composites, are of interest due to their high-temperature strength. The quasi-binary eutectic reactions between 'fcc-carbides' with the NaCl-type structure (e.g. TaC) and chromium-based bcc-phases of the ternary C–Cr–M systems (M is a d-metal of groups IV–VIII in the periodic table) have been studied rather comprehensively [1]. At present, for the C–Cr–M alloys, their most important applications are the as-cast and sintered chromium alloys with a d-metal carbide as the dispersion-strengthening phase, the cast alloys based on chromium-carbide eutectics (especially (Cr)+(TiC)), and sintered composites based on chromium carbides with a binder whose principal component is a metal of the iron group (for instance, the materials based on Cr_3C_2 with a KKhN nickel binder) [2]. It was reported that the hardness of the eutectic alloy (Cr)+(TaC) is higher than that of the eutectic alloy (Cr)+(TiC) [3].

Information on the phase equilibria in the C–Cr–M systems is essential to solve practical problems in the development of the new materials and define the conditions for the production of these materials and subsequent heat treatment to obtain optimal engineering properties. Thermodynamic description is also needed to obtain the thermodynamic factor via the CALPHAD approach for the development of the diffusion database. So far, no thermodynamic description of the C–Cr–Ta system is available in the literature. In the present work, a thermodynamic optimization for the C–Cr–Ta ternary system is performed based on the experimental phase diagram data in the literature.

2. Evaluation of experimental phase diagram data in the C–Cr–Ta system

The phase equilibria of the C–Cr–Ta ternary system at 1000 and 1350 °C were investigated by Fedorov et al. [4] and Rassaerts et al. [5], respectively. The phase relationships on the published isothermal sections at 1000 and 1350 °C do not show any major differences. It could be deduced that the phase relationships in the system remain unchanged in the temperature range from 1000 °C to the solidus, considering the report by Velikanova et al. [6]. It should be mentioned that the homogeneity range of TaC on the binary side of the 1000 °C isothermal section published by Fedorov et al. [4] is quite different from that in the currently accepted C–Ta phase diagram [7]. The latter [7] is accepted in the present modeling of the C–Cr–Ta ternary system. However, the topology phase relationships established by Fedorov et al. [4] are used as reliable experimental data in the present thermodynamic optimization.

The solidus temperatures of the C–Cr–Ta system were determined by Velikanova et al. [6] using the Pirani–Alterthum method. It was revealed that the thermodynamically most stable fcc-carbide (TaC) is predominant in the phase equilibria of the C–Cr–Ta system at the solidus temperatures. The TaC phase, which has the largest homogeneity region, is in equilibrium with all the phases in the ternary system, except for the (Ta) phase. Velikanova et al. [6] pointed out that this carbide forms quasi-binary eutectics with the

* Corresponding author at: Research Institute of Powder Metallurgy, Central South University, Changsha, Hunan 410083, PR China. Tel.: +86 731 88836213; fax: +86 731 88710855.
E-mail address: yongducalphad@gmail.com (Y. Du).

0925-8388/$ – see front matter © 2011 Elsevier B.V. All rights reserved.
doi:10.1016/j.jallcom.2011.01.202

Cr_7C_3 and ($\beta TaCr_2$), which melt congruently. Three maximum temperature points were observed on the liquidus projection, which are $L \leftrightarrow$ (TaC) + ($\beta TaCr_2$) at 1990 °C, $L \leftrightarrow$ (TaC) + Cr_7C_3 at 1720 °C and $L \leftrightarrow$ (TaC) + (Cr) at 1683 °C.

Afterwards, Velikanova et al. [8] determined the phase boundaries of the phases involved in the invariant equilibria by electron probe micro-analyses (EPMA). The fields of primary crystallization for the phases were established with metallography and EPMA. They suggested the existence of another maximum temperature point for $L \leftrightarrow$ (Ta_2C) + ($\beta TaCr_2$) above 1960 °C. Nevertheless, this conclusion is contradictory to their previously reported maximum temperature point for $L \leftrightarrow$ (TaC) + ($\beta TaCr_2$) [4], the existence of which was not confirmed by their subsequent investigation [8].

The quasi-binary eutectic of (Cr) + (TaC) reported by Velikanova et al. [6,8] was reinvestigated by Dovbenko et al. [3]. Based on the differential thermal analysis (DTA) curves of the alloys including the arrests that correspond to three-phase eutectics, the reaction temperature of $L \leftrightarrow$ (TaC) + (Cr) was concluded to be about 1690 °C. They suggested that the maximum temperature point is shallow and located between the alloys $Cr_{79.9}Ta_{12.8}C_{7.3}$ and $Cr_{79.5}Ta_{11.5}C_9$, and the $Cr_{82.5}Ta_{10}C_{7.5}$ alloy is close to the quasi-binary eutectic.

3. Thermodynamic models

In the present modeling, the Gibbs energy functions for C, Cr and Ta were from the SGTE compilation by Dinsdale [9]. The thermodynamic parameters in the C–Cr, C–Ta, and Cr–Ta systems were taken from Refs. [10,7,11], respectively. The sublattice model [12,13] was used to describe the binary phases extending into the ternary system. In view of the experimental data [4–6] that the solid solubility of Ta in the C–Cr binary compounds ($Cr_{23}C_6$, Cr_7C, Cr_3C_2) and the solubility of C in the Cr–Ta binary compounds (($\alpha TaCr_2$), ($\beta TaCr_2$)) are small, all of them are treated as pure binary ones.

3.1. Binary systems

3.1.1. The C–Cr system

Many researchers [14–18] have determined the phase equilibria of the C–Cr system by DTA and Pirani black body hole techniques. The thermodynamic modeling for this system was performed firstly by Andersson [19], and updated by Kajihara and Hillert [20] taking into account the emf (electron motive force) data published by Du et al. [21]. The thermodynamic parameters obtained by these two groups of authors, however, could not meet the demand for a reasonable extrapolation to the Fe–Cr–V–C system. Consequently, Lee [10] reassessed the C–Cr system by taking into account the extrapolation to the C–Cr–Ni system as well as Fe–Cr–V–C system. The parameters published by Lee [10] were regarded to be most suitable for the C–Cr system. Though, a reassessment of this system was carried out by Teng et al. [22] using the new emf data for the Cr_3C_2 phase, their results are close to those obtained by Lee [10]. Thus the modeling by Lee [10] is adopted in the present modeling, and the calculated phase diagram [10] is reproduced in Fig. 1. The differences between the measured and the calculated phase diagram for the the C–Cr binary system have been discussed in detail by Schuster and Du [23].

3.1.2. The C–Ta system

The establishment of the C–Ta phase diagram is mainly due to three groups of authors [24–26]. The thermodynamic modeling of the C–Ta system was conducted by Frisk and Guillermet [7]. The complete thermodynamic description of the C–Ta system [7] was used to describe the ternary system Ta–C–N [27], resulting in an excellent agreement with the experimental data. Consequently, the parameters from Frisk and Guillermet [7] were accepted in the present modeling, as shown in Fig. 2.

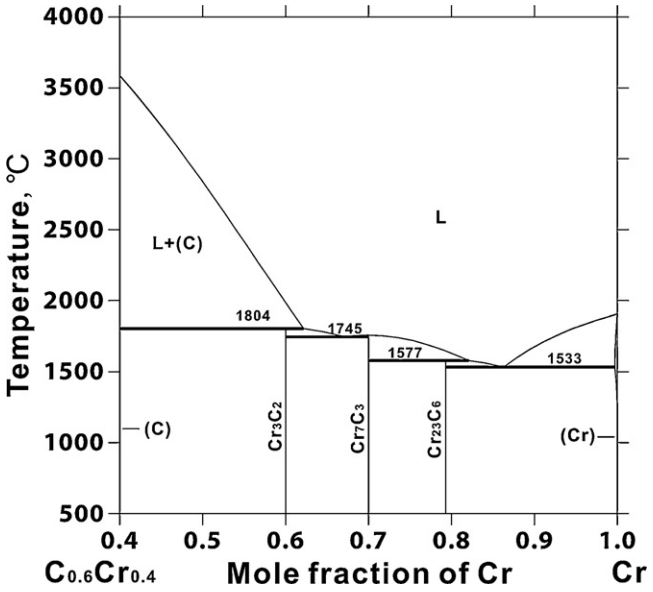

Fig. 1. Calculated C–Cr phase diagram according to Lee [10].

3.1.3. The Cr–Ta system

The first contribution to the Cr–Ta phase diagram was made by Kubaschewski et al. [28,29]. Subsequently, this system was investigated by Gebhardt and Rexer [30], Rudy [31] and Kocherzhinsky et al. [32]. Based on these experimental data, a set of self-consistent thermodynamic parameters for the Gibbs energies of individual phases in the Cr–Ta system was obtained by Dupin and Ansara [33]. Most recently, a remodeling of the Laves phases (($\alpha TaCr_2$), ($\beta TaCr_2$)) in the Cr–Ta system was conducted by Pavlu et al. [11] using the results from the first-principles calculation. As shown in Fig. 3, the calculated composition range of the ($\alpha TaCr_2$) phase (in solid lines) according to Pavlu et al. [11] is considerably larger than Dupin's results. Due to the better extrapolation to the 1000 °C [4] and the 1350 °C [5] isothermal sections in the C–Cr–Ta ternary system, the Pavlu's thermodynamic parameters for the Cr–Ta system [11] are accepted in the present modeling and the calculated Cr–Ta phase diagram is reproduced in Fig. 3.

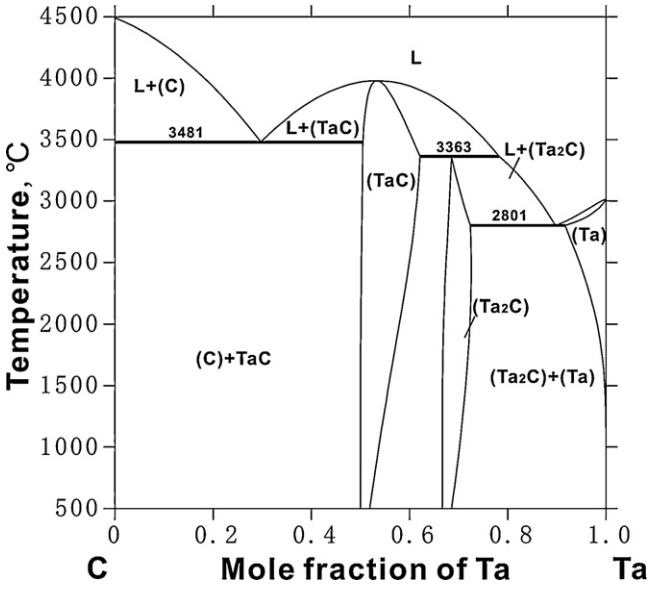

Fig. 2. Calculated C–Ta phase diagram according to Frisk and Guillermet [7].

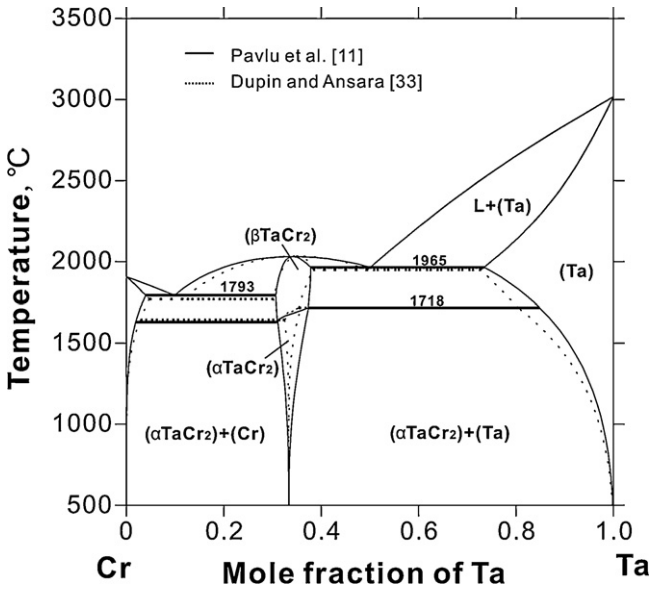

Fig. 3. Calculated Cr–Ta phase diagram according to Pavlu et al. [11] compared with Dupin and Ansara [33].

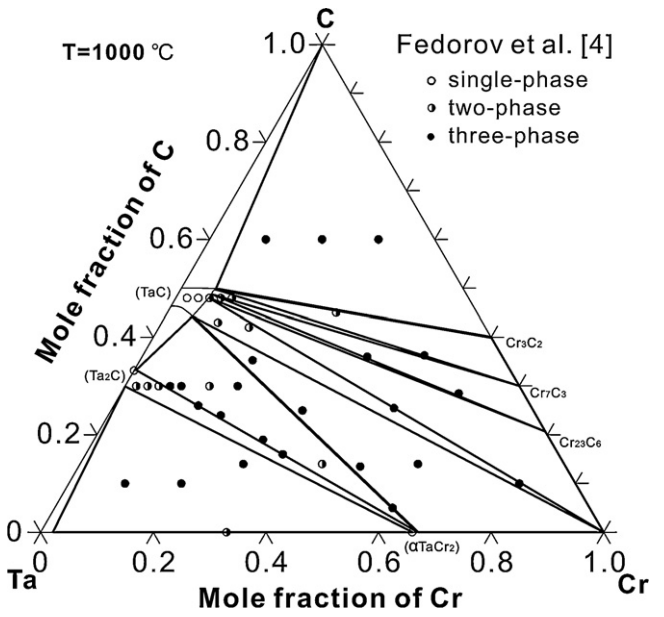

Fig. 4. Calculated isothermal section at 1000 °C of the C–Cr–Ta system, compared with the experimental data reported by Fedorov et al. [4].

3.2. Solution phase

3.2.1. Liquid phase

The liquid phase is described using a substitional solution model, $(C, Cr, Ta)_1$. The Gibbs energy per mole of atom is given by:

$$ {}^0G_m^L = x_C {}^0G_C^L + x_{Cr} {}^0G_{Cr}^L + x_{Ta} {}^0G_{Ta}^L + RT(x_C \ln x_C + x_{Cr} \ln x_{Cr} + x_{Ta} \ln x_{Ta}) + {}^{ex}G_m^L \quad (1) $$

where x_i is the mole fraction of element i and ${}^0G_i^L$ the Gibbs energy of element i in the liquid form. The second term in Eq. (1) is the ideal entropy of mixing and the third term is the excess Gibbs energy.

For the liquid phase, the excess Gibbs energy is described by the Redlich–Kister polynomial [34]:

$$ {}^{ex}G_m^L = x_C x_{Cr} L_{C,Cr}^L + x_C x_{Ta} L_{C,Ta}^L + x_{Cr} x_{Ta} L_{Cr,Ta}^L + x_C \cdot x_{Cr} \cdot x_{Ta} \cdot (x_C \cdot {}^0L_{C,Cr,Ta}^L + x_{Cr} \cdot {}^1L_{C,Cr,Ta}^L + x_{Ta} \cdot {}^2L_{C,Cr,Ta}^L) \quad (2) $$

where ${}^0L_{C,Cr,Ta}^L$, ${}^1L_{C,Cr,Ta}^L$ and ${}^2L_{C,Cr,Ta}^L$ are ternary parameters to be evaluated in the present work. The parameters denoted as $L_{i,j}^L$ are the interaction parameters from the binary systems.

3.2.2. fcc, bcc and hcp phases

The fcc, bcc and hcp phases are described by a two-sublattice model $(Cr, Ta)_1(C, Va)_n$. The Cr and Ta atoms can substitute for each other on the metal sublattice and the carbon and vacancy (Va) on the interstitial sublittice. The symbol n denotes the number of interstitial sites per metal atom. In the case of fcc, n is equal to 1 for crystallographic reasons. If ϕ denotes the phase, the Gibbs energy per mole of formula unit of $(Cr, Ta)_1(C, Va)_n$ is given by:

$$ \begin{aligned} {}^0G^\phi &= y'_{Cr} \cdot y''_C \cdot {}^0G^\phi_{Cr:C} + y'_{Cr} \cdot y''_{Va} \cdot {}^0G^\phi_{Cr:Va} + y'_{Ta} \cdot y''_C \cdot {}^0G^\phi_{Ta:C} \\ &+ y'_{Ta} \cdot y''_{Va} \cdot {}^0G^\phi_{Ta:Va} + RT \cdot (y'_{Cr} \ln y'_{Cr} + y'_{Ta} \ln y'_{Ta}) \\ &+ n \cdot RT(y''_C \ln y''_C + y''_{Va} \ln y''_{Va}) + y'_{Cr} y''_C y''_{Va} \cdot L^\phi_{Cr:C,Va} \\ &+ y'_{Ta} y''_C y''_{Va} \cdot L^\phi_{Ta:C,Va} + y'_{Cr} y'_{Ta} y''_{Va} \cdot L^\phi_{Cr,Ta:Va} + y'_{Cr} y'_{Ta} y''_C \cdot L^\phi_{Cr,Ta:C} \\ &+ y'_{Cr} y'_{Ta} y''_C y''_{Va} \cdot L^\phi_{Cr,Ta:C,Va} \end{aligned} \quad (3) $$

in which y'_{Cr} and y'_{Ta} are the site fractions of the Cr and Ta on the first sublattice, y''_C and y''_{Va} are the site fraction of C and Va on the second one. The ternary parameters $L^\phi_{Cr,Ta:C}$ and $L^\phi_{Cr,Ta:C,Va}$ were optimized in this study.

4. Results and discussion

The model parameters were evaluated using the computer-operated optimization program PARROT [35], which works by minimizing the sum of square of the differences between measured and calculated values.

The optimization began with the phase (TaC). Using the experimental phase equilibrim data for the (TaC) phase at 1350 °C [5], the ternary parameters were assessed for this phase and then fixed during the subsequent optimization steps. Secondly, the (Ta_2C) phase was included in the optimization. Using the experimental solubility data for the Cr in the (Ta_2C) phase at 1000 °C [4]

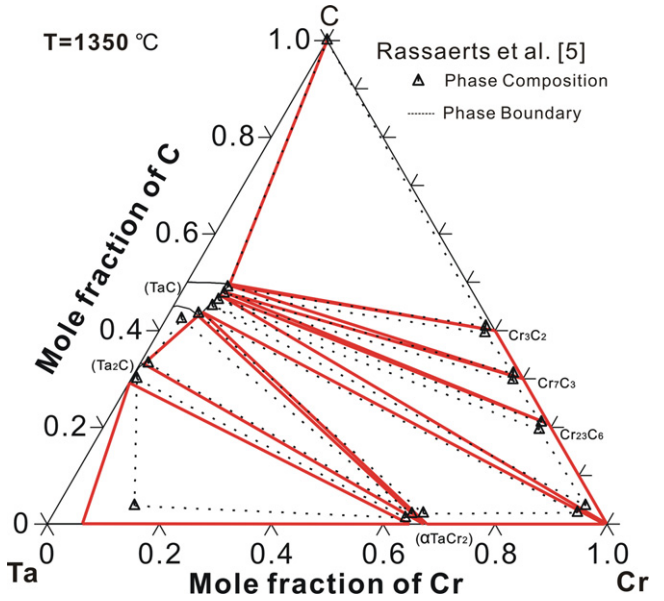

Fig. 5. Calculated isothermal section at 1350 °C of the C–Cr–Ta system, compared with the experimental data reported by Rassaerts et al. [5].

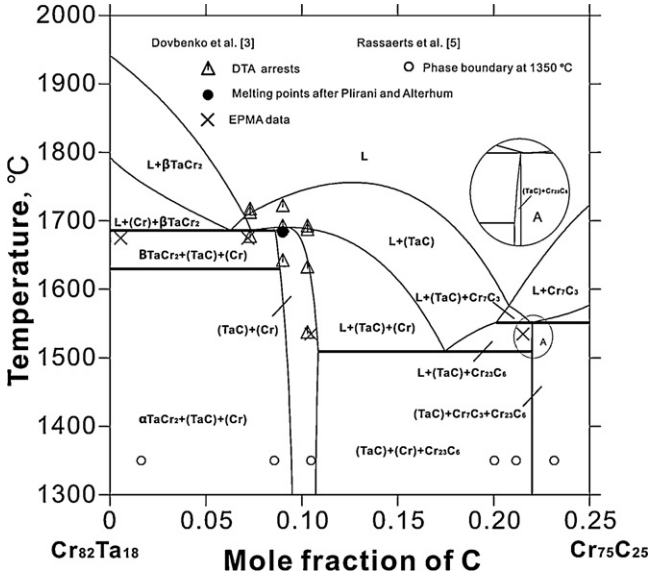

Fig. 6. Calculated $Cr_{82}Ta_{18}$–$Cr_{75}C_{25}$ vertical section of the C–Cr–Ta system, compared with the experimental data reported by Dovbenko et al. [3] and Rassaerts et al. [5].

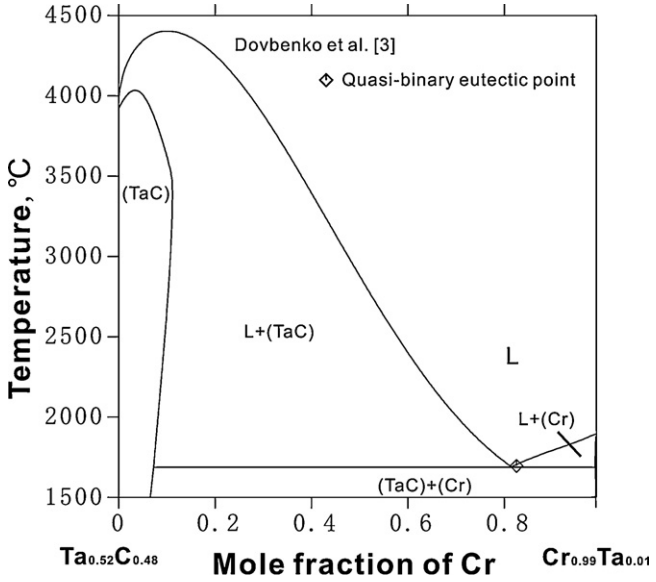

Fig. 8. Calculated quasi-binary eutectic reaction $L \leftrightarrow (TaC)+(Cr)$ of the C–Cr–Ta system, compared with the experimental data reported by Dovbenko et al. [3].

and 1350 °C [5], a constant regular parameter was assessed. The regular interaction parameters for the liquid phase were then adjusted in order to reproduce the experimental data on the invariant reactions [6], two vertical sections [3,8], solidus surface [6] and liquidus surface [3] of the C–Cr–Ta system. Finally, the thermodynamic parameters for all the phases were optimized simultaneously by taking into account all of the selected phase diagram data.

The thermodynamic parameters describing the C–Cr–Ta system are given in Table 1. The parameters assessed in the present work are underlined. Using this set of parameters, a series of phase diagrams, including isothermal sections, vertical sections, and the projection of the solidus surface and liquidus surface are calculated to account for the rationality of this thermodynamic description.

Table 2 compares the calculated invariant reaction temperatures and liquid compositions with the experimental observations [3,6,8]. A good agreement is obtained for most of the established invariant reaction temperatures. However, the presently calculated temperatures for the invariant reactions U_3 and E_4 are noticeably different from the experimental ones. These discrepancies are due to the fact that the thermodynamic parameters for the C–Cr binary system [10], which were used in the present work, were obtained based on the experimental data measured by Rudy [14] and Knotek et al. [15] rather than the researchers [3,6,8] utilized one [16]. The temperatures determined by Eremenko et al. [16] for the invariant reactions $L \leftrightarrow Cr_{23}C_6 + (Cr)$ and $L + Cr_7C_3 \leftrightarrow Cr_{23}C_6$ are about 40 °C higher than the ones determined by Rudy [14] and Knotek et al. [15]. From the paper published by Velikanova et al. [8], we found that the determined invariant temperatures in the C–Cr–Ta system have been amended by the researchers [3,6,8] according to Eremenko et al. [16]. This can explain why

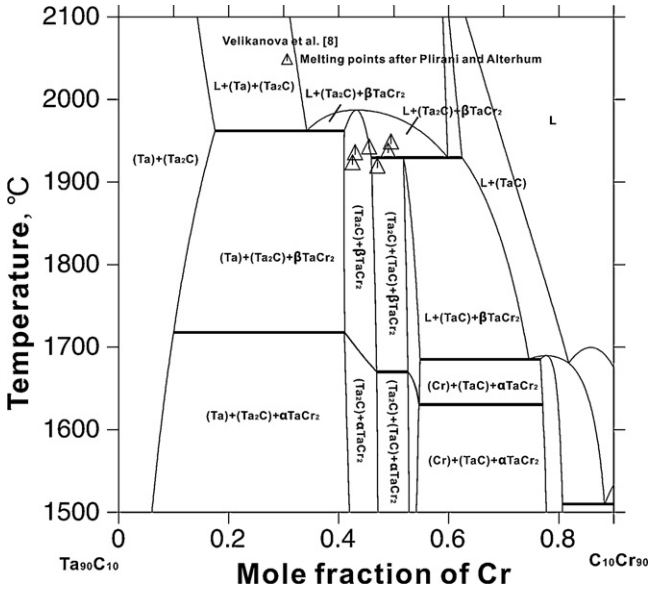

Fig. 7. Calculated vertical section at 10 at.% C of the C–Cr–Ta system, compared with the experimental data reported by Velikanova et al. [8].

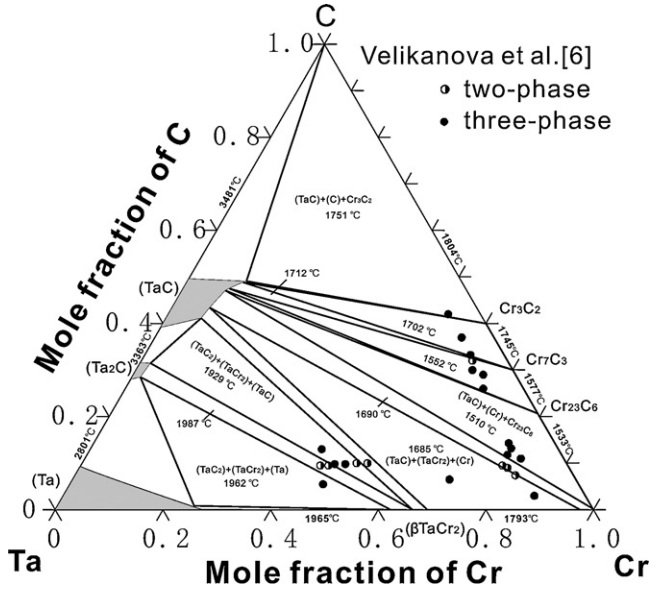

Fig. 9. Calculated solidus surface of the C–Cr–Ta system, compared with the experimental data reported by Velikanova et al. [6], the temperatures marked in different regions are the start melting temperature for the alloys in each region.

Table 1
Thermodynamic parameters in the C–Cr–Ta system[a].

Liquid: Model $(C,Cr,Ta)_1$

$^0L^{Liq}_{C,Cr} = -90,526 - 25.9116T$, $^1L^{Liq}_{C,Cr} = 80,000$, $^2L^{Liq}_{C,Cr} = 80,000$

$^0L^{Liq}_{C,Ta} = -173413.25 - 7.1858T$, $^1L^{Liq}_{C,Ta} = 23643.16$

$^0L^{Liq}_{Cr,Ta} = -18,600 + 6.2T$, $^1L^{Liq}_{Si,Zn} = 12,600 - 4.2T$

$^0L^{Liq}_{C,Cr,Ta} = \underline{-1,112,430}$, $^1L^{Liq}_{C,Cr,Ta} = \underline{-159,819}$, $^2L^{Liq}_{C,Cr,Ta} = \underline{490,000}$

(Cr,Ta)-bcc: Model $(Cr,Ta,Va)_1(C,Va)_3$

$^0G^{bcc}_{Cr:C} - {}^0G^{bcc}_{Cr} - 3{}^0G^{gra}_{C} = 416,000$, $^0L^{bcc}_{Cr:C,Va} = -190T$

$^0G^{bcc}_{Ta:C} - {}^0G^{bcc}_{Ta} - 3{}^0G^{gra}_{C} = 601379.32 - 61.1233T$, $^0L^{bcc}_{Ta:C,Va} = -749073.01$

$^0L^{bcc}_{Cr,Ta:Va} = 46,800 - 11.4T$, $^1L^{bcc}_{Cr,Ta:Va} = 37,200 - 17.3T$, $^2L^{bcc}_{Cr,Ta:Va} = 16,200 - 5.4T$

(TaC)-fcc: Model $(Cr,Ta)_1(C,Va)_1$

$^0G^{fcc}_{Cr:C} - {}^0G^{bcc}_{Cr} - {}^0G^{gra}_{C} = 1200 - 1.94T$, $^0L^{fcc}_{Cr:C,Va} = -11,977 + 6.8194T$

$^0G^{fcc}_{Ta:C} - H^{SER}_{C} - H^{SER}_{Ta} = -163834.55 + 266.90346T - 44.957558T\ \ln(T) - 0.0036198T^2 + 594677.55T^{-1} - 2.310674 \times 10^9 T^{-3} + 1.9237 \times 10^{13} T^{-5} - 3.5155676 \times 10^{16} T^{-7}$

$^0L^{fcc}_{Ta:C,Va} = -60408.461 + 4.17256T$

$^0L^{fcc}_{Cr,Ta:C} = \underline{217,894 - 125T}$, $^2L^{fcc}_{Cr,Ta:C} = \underline{-499,846 + 125T}$

$^0L^{fcc}_{Cr,Ta:C,Va} = \underline{250,000}$, $^1L^{fcc}_{Cr,Ta:C,Va} = \underline{-650,000}$

(Ta_2C)-hcp: Model $(Cr,Ta)_1(C,Va)_{0.5}$

$^0G^{hcp}_{Cr:C} - {}^0G^{bcc}_{Cr} - 0.5{}^0G^{gra}_{C} = 18,504 + 9.4176T - 2.4997T\ \ln(T) + 0.001386T^2$, $^0L^{hcp}_{Cr:C,Va} = 4165$

$^0G^{hcp}_{Ta:C} - 0.5H^{SER}_{C} - H^{SER}_{Ta} = -107522.86 + 142.266T - 26.879883T\ \ln(T) - 0.0057393884T^2$

$^0L^{hcp}_{Ta:C,Va} = -6917.5538$

$^0L^{hcp}_{Cr,Ta:C} = \underline{20,000}$

($\alpha TaCr_2$)-Laves_C15: Model $(Cr,Ta)_2(Cr,Ta)_1$

$^0G^{\alpha TaCr_2}_{Cr:Cr} - 3{}^0G^{bcc}_{Cr} = 81,870$, $^0G^{\alpha TaCr_2}_{Ta:Ta} - 3{}^0G^{fcc}_{Ta} = 32,820$

$^0G^{\alpha TaCr_2}_{Ta:Cr} - {}^0G^{bcc}_{Cr} - 2{}^0G^{bcc}_{Ta} = 223,170 - 0.65T$ $^0G^{\alpha TaCr_2}_{Cr:Ta} - 2{}^0G^{bcc}_{Cr} - {}^0G^{bcc}_{Ta} = -33,870 + 2.53T$

$L^{\beta TaCr_2}_{Cr,Ta:Cr} = 240,000$, $L^{\beta TaCr_2}_{Cr:Cr,Ta} = -35,000 - 9.85T$

$L^{\beta TaCr_2}_{Ta:Cr,Ta} = 79,000$, $L^{\beta TaCr_2}_{Cr,Ta:Ta} = 55,000 + 4.95T$

($\beta TaCr_2$)-Laves_C14: Model $(Cr,Ta)_2(Cr,Ta)_1$

$^0G^{\beta TaCr_2}_{Cr:Cr} - 3{}^0G^{bcc}_{Cr} = 85,890$, $^0G^{\beta TaCr_2}_{Ta:Ta} - 3{}^0G^{fcc}_{Ta} = 28,050$

$^0G^{\beta TaCr_2}_{Ta:Cr} - {}^0G^{bcc}_{Cr} - 2{}^0G^{bcc}_{Ta} = 229,050 + .112T$ $^0G^{\beta TaCr_2}_{Cr:Ta} - 2{}^0G^{bcc}_{Cr} - {}^0G^{bcc}_{Ta} = -30,750 + 0.999T$

$L^{\beta TaCr_2}_{Cr,Ta:Cr} = 79,000$, $L^{\beta TaCr_2}_{Cr:Cr,Ta} = -2500 - 23.4T$

$L^{\beta TaCr_2}_{Ta:Cr,Ta} = 240,000$, $L^{\beta TaCr_2}_{Cr,Ta:Ta} = 80,400 - 10.3T$

C: Model $(C)_1$

$Cr_{23}C_6$: Model $Cr_{23}C_6$

$^0G^{Cr_{23}C_6}_{Cr:C} - 23{}^0G^{bcc}_{Cr} - 6{}^0G^{gra}_{C} = -521,983 + 3622.24T - 620.965T\ \ln(T) - 0.126431T^2$

Cr_7C_3: Model Cr_7C_3

$^0G^{Cr_7C_3}_{Cr:C} - 7{}^0G^{bcc}_{Cr} - 3{}^0G^{gra}_{C} = -201,690 + 1103.128T - 190.177T\ \ln(T) - 0.0578207T^2$

Cr_3C_2: Model Cr_3C_2

$^0G^{Cr_3C_2}_{Cr:C} - 3{}^0G^{bcc}_{Cr} - 2{}^0G^{gra}_{C} = -100823.8 + 530.66989T - 89.6694T\ \ln(T) - 0.0301188T^2$

[a] In J/(mol of atom). The Gibbs energies for the pure elements are from the SGTE compilation. The thermodynamic parameters in the C–Cr, C–Ta and Cr–Ta systems are taken from Lee [10], Frisk and Guillermet [7] and Pavlu et al. [11], respectively. Only the underlined parameters are assessed in the present work.

the experimental temperature of the ternary eutectic reaction $L \leftrightarrow (TaC) + Cr_{23}C_6 + (Cr)$ at 1542 °C is even higher than that of the binary eutectic reaction $L \leftrightarrow Cr_{23}C_6 + (Cr)$ at 1533 °C calculated by Lee [10]. Consequently, the calculated invariant reaction temperatures for the invariant reactions U_3 and E_4 according to present thermodynamic description are acceptable. Taking account into all of the experimental data including the liquidus projection and invariant reaction temperatures, the value of $^2L^{Liq}_{C,Cr,Ta}$ was fixed at 490,000

Table 2
Comparison of the calculated and measured invariant reaction temperatures and the liquid phase compositions in the C–Cr–Ta system.

Reaction	Composition (at.% Cr, at.% C)		T (°C)	Reference
$L \leftrightarrow (\beta TaCr_2) + (Ta_2C)$, e_3	58.6	2.0	≥1960	[8]
			1987	This work
$L \leftrightarrow (Ta_2C) + (TaCr_2) + (Ta)$, E_1	50.9	0.5	1935±7	[8]
			1962	This work
$L + (Ta_2C) \leftrightarrow (TaC) + (\beta TaCr_2)$, U_1	>67.5	6	1943 ± 21	[8]
	67.6	7.1	1930	This work
$L + (C) \leftrightarrow (TaC) + Cr_3C_2$, U_2	56.6	39.3	1748 ± 5	[6]
			1751	This work
$L \leftrightarrow (TaC) + Cr_7C_3$, e_8	64.7	31.6	1720	[6]
			1712	This work
$L \leftrightarrow (TaC) + Cr_3C_2 + Cr_7C_3$, E_2	64.8	31.5	1704 ± 4	[6]
			1702	This work
$L \leftrightarrow (TaC) + (Cr)$, e_9	82.5	7.5	≥1690	[3]
	81.5	8.4	1690	This work
$L \leftrightarrow (TaC) + (Cr) + (\beta TaCr_2)$, E_3	81.1	6.8	1675 ± 8	[3]
			1685	This work
$L + Cr_7C_3 \leftrightarrow (TaC) + Cr_{23}C_6$, U_3	77.6	19.6	1576 ± 16	[3]
			1552	This work
$L \leftrightarrow (TaC) + Cr_{23}C_6 + (Cr)$, E_4	82.1	15.3	1542 ± 6	[3]
			1510	This work

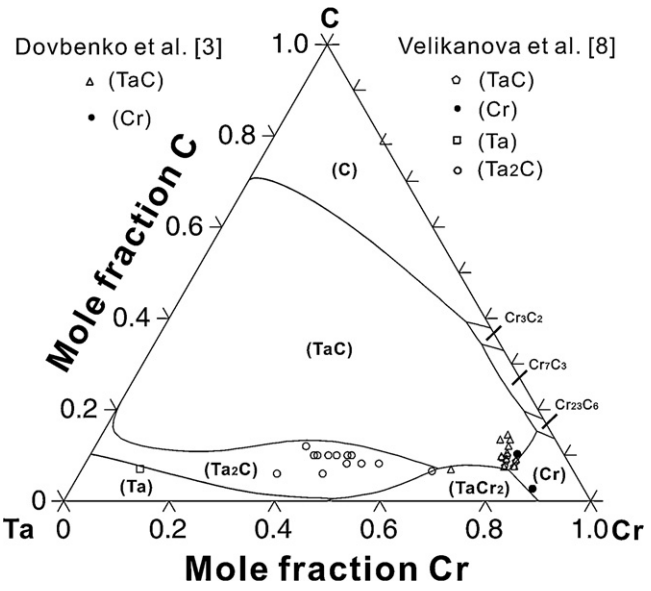

Fig. 10. Calculated liquidus surface of the C–Cr–Ta system, compared with the experimental data reported by Dovbenko et al. [3] and Velikanova et al. [8].

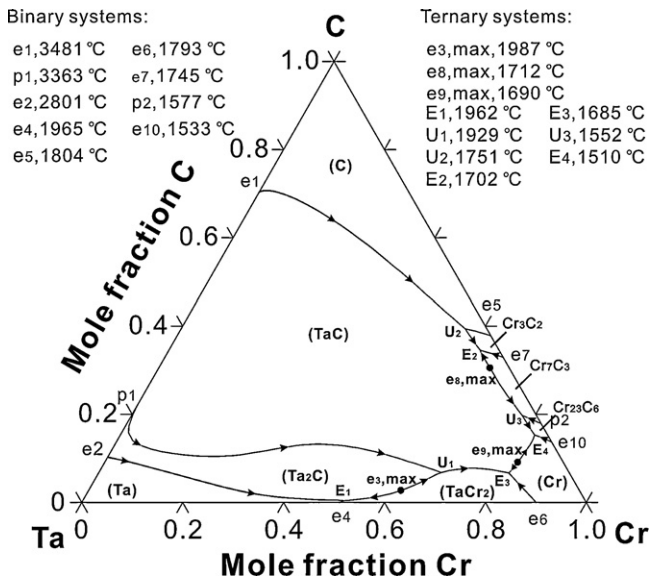

Fig. 12. Calculated liquidus projection of the C–Cr–Ta system together with the temperatures of invariant reactions.

in the present modeling. However, the large value of the parameter ${}^{2}L^{\mathrm{Liq}}_{\mathrm{C,Cr,Ta}}$ led to that the calculated invariant temperature for the invariant reaction E_1 is about 25 K higher than the experimental one.

Figs. 4 and 5 show the calculated isothermal sections at 1000 °C and 1350 °C of the C–Cr–Ta system, compared with experimental data reported by Fedorov et al. [4] and Rassaerts et al. [5], respectively. The experimental data reported by Fedorov et al. [4] are not utilized in the present optimization but used for a comparison. As shown in Fig. 5, the agreement between the present thermodynamic description and Rassaerts's [5] results is very well.

Fig. 6 presents the calculated $Cr_{82}Ta_{18}$–$Cr_{75}C_{25}$ vertical section of the C–Cr–Ta system, compared with the experimental data reported by Dovbenko et al. [3] and Rassaerts et al. [5]. Good agreement is obtained between the present thermodynamic description and experimental data. As shown in Fig. 6, we can also find that the maximum of $L \leftrightarrow$ (TaC) + (Cr) is shallow, which is reported by Dovbenko et al. [3]. Fig. 7 is calculated vertical section at 10 at.% C of the C–Cr–Ta system, compared with the experimental data reported by Velikanova et al. [8].

Fig. 8 compares the calculated quasi-binary eutectic reaction $L \leftrightarrow$ (TaC) + (Cr) of the C–Cr–Ta system with the experimental data reported by Dovbenko et al. [3]. As can be seen in Fig. 8, the calculated temperature of $L \leftrightarrow$ (TaC) + (Cr) is 1690 °C, which fits very well with the measured one, and the calculated liquid composition is $Cr_{81.5}Ta_{10.1}C_{8.4}$, which is very close to $Cr_{82.5}Ta_{10}C_{7.5}$ determined by Dovbenko et al. [3].

Fig. 9 presents the calculated solidus surface of the C–Cr–Ta system, compared with the experimental data reported by Velikanova et al. [6]. As shown in Fig. 9, the calculated results fit well with the experimental data.

Fig. 10 presents calculated liquidus surface of the C–Cr–Ta system, compared with the experimental data reported by Velikanova et al. [8] and Dovbenko et al. [3]. As can be seen in Fig. 10, the present thermodynamic description can reproduce the primary phases of alloys determined by Velikanova et al. [8] and Dovbenko et al. [3]. Fig. 11 shows the calculated liquidus projections in the Cr-rich corner, compared with the experimental data reported by Dovbenko et al. [3]. Good agreement is obtained between calculation and experiment.

Using the parameters assessed in the present work, the calculated liquidus and solidus projections of the C–Cr–Ta system together with the temperatures of invariant reactions are presented in Fig. 12. Finally the reaction scheme for the C–Cr–Ta system is shown in Fig. 13.

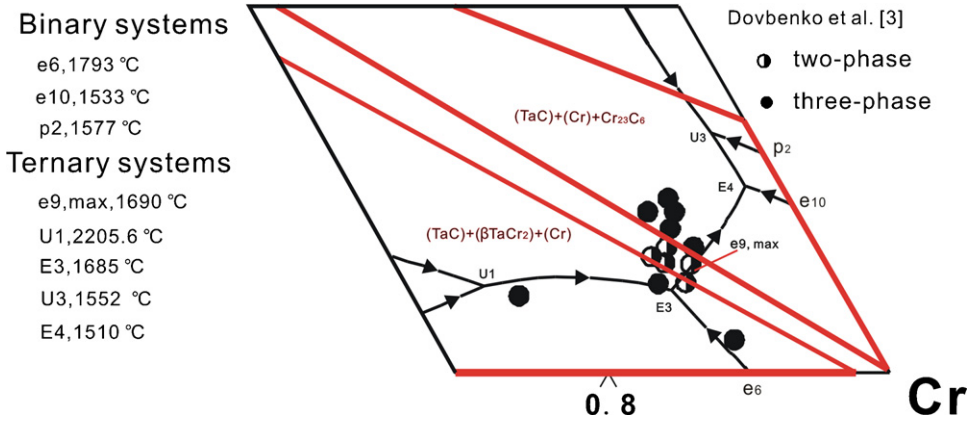

Fig. 11. Calculated liquidus and solidus surfaces of the C–Cr–Ta system in the Cr-rich corner, compared with the experimental data reported by Dovbenko et al. [3].

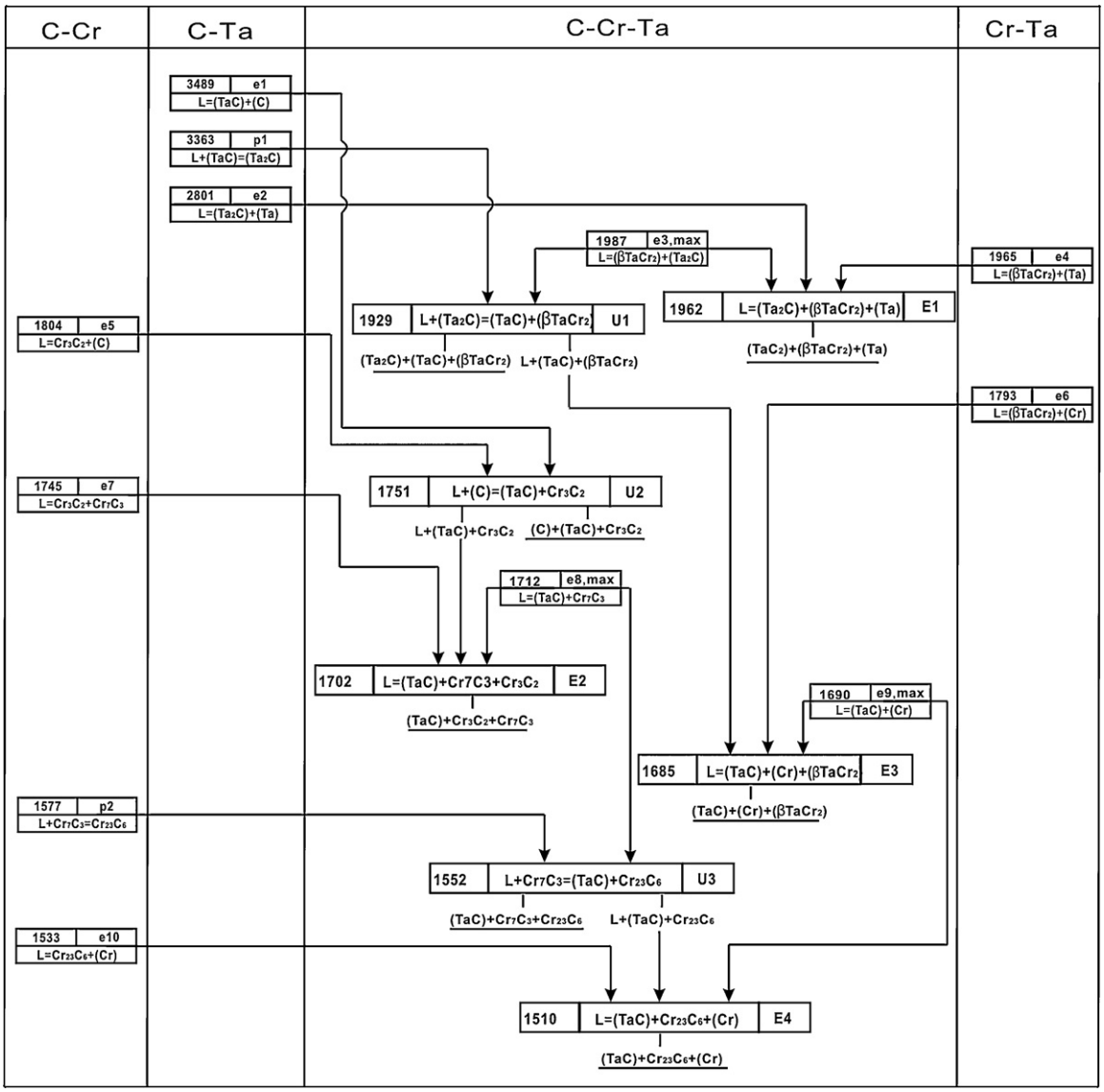

Fig. 13. Reaction scheme of the C–Cr–Ta system according to the present calculation. Temperature is in °C.

5. Summary

The phase equilibrium data in the C–Cr–Ta system available in the literature were critically reviewed. On the basis of reliable experimental data, a thermodynamic description of the ternary system was developed. Comprehensive comparisons show that most of the experimental data are well accounted for by the present description.

The liquidus projection and reaction scheme of the C–Cr–Ta system over wide temperature and composition ranges were presented, which is of interest for practical applications as well as basic materials research.

Acknowledgements

The financial support from the Creative Research Group of National Natural Science Foundation of China (Grant No. 50721003), the key program of the National Natural Science Foundation of China (Grant No. 50831007 and 20833009) and China Zhuzhou Cemented Carbide Cutting Tools Co., LTD is acknowledged.

References

[1] A.A. Bondar, T.Ya. Velikanova, Powder Metall. Metal. Ceram. 35 (7–8) (1996) 484–496, Translated from Poroshk. Metall. (Kiev) (7–8) (1996) 182–192.
[2] V.N. Antsiferov, V.D. Khramtsov, Powder Metall. Metal. Ceram. 42 (11–12) (2003) 603–606.
[3] O.I. Dovbenko, A.A. Bondar, T.Ya. Velikanova, O.O. Bilous, M.P. Burka, P.S. Martseniuk, T.O. Shapoval, N.I. Tsyganenko, Mater. Lett. 57 (19) (2003) 2866–2871.
[4] T.F. Fedorov, N.M. Popova, L.V. Gorshkova, T.R.V. Skolozdra, Yu.B. Kuz'ma, Sov, Powder Metall. Metal. Ceram. 7 (11) (1968) 193–197, Translated from Poroshk. Metall. (Kiev) (11) (1968) 42–48.
[5] H. Rassaerts, F. Benesovsky, H. Novotny, Planseeber. Pulver-metall 13 (3) (1965) 199–206.
[6] T.Ya. Velikanova, A.A. Bondar, A.V. Grytsiv, O.I. Dovbenko, J. Alloys Compd. 320 (2001) 341–352.
[7] K. Frisk, A.F. Guillermet, J. Alloys Compd. 238 (1996) 167–179.
[8] T.Ya. Velikanova, A.A. Bondar, O.I. Dovbenko, Powder Metall. Metal. Ceram. 41 (7–8) (2002) 400–406.
[9] A.T. Dinsdale, CALPHAD 15 (1991) 317–425.
[10] B.J. Lee, CALPHAD 16 (1992) 121–149.
[11] J. Pavlu, J. Vrestal, M. Sob, CALPHAD 33 (2009) 179–186.
[12] M. Hillert, L.I. Staffansson, Acta Chem. Stand. 24 (1970) 3618–3626.
[13] B. Sundman, J. Agren, J. Phys. Chem. Solids 42 (1981) 297–301.
[14] E. Rudy, Technical Report No. AFML–TR–65-2, 1969, pp. 179–180.
[15] O. Knotek, E. Lugscheider, H. Reimann, H.G. Sasse, Metall 35 (1981) 130–132.
[16] V.N. Eremenko, T. Velikanova, A.A. Bondar, Poroshk. Metall. 5 (1987) 70–76.
[17] V. Ivanchenko, V. Gridnev, V. Pogorelajo, Dep. VINITI 29.06.89, N4293-BS9, Kiev, Ukraine (1989).

[18] Y.J. Bhatt, R. Venkataramani, Y.S. Sayi, S.P. Garg, Met. Mater. Process. 2 (1990) 49–57.
[19] J.-O. Andersson, CALPHAD 11 (1987) 271–276.
[20] M. Kajihara, M. Hillert, Metall. Trans. 21A (1990) 2777–2787.
[21] S.H. Du, S. Seetharaman, L.–I. Staffansson, Metall. Trans. B 20B (1989) 911–917.
[22] L.D. Teng, X.G. Lu, R.E. Aune, S. Seetharaman, Metall. Trans. 35A (2004) 3673–3680.
[23] J.C. Schuster, Y. Du, CALPHAD 23 (1999) 393–408.
[24] E. Rudy, D.E. Harmon, Technical Rep. No. AFML–TR–65-2, Part I, vol. V, 1966 (Aerojet General Corp.).
[25] C.F. Zalabak, Technical Note TN D–761, 1961 (NASA).
[26] R.V. Sara, C.E. Lowell, WADD TDR–60-143, Part V, 1964 (Wright Air Develop., Div., Wright–Patterson A.F.B., OH).
[27] K. Frisk, J. Alloys Compd. 278 (1996) 216–226.
[28] O. Kubaschewski, A. Schneider, J. Inst. Met. 75 (1948–1949) 403–416.
[29] O. Kubaschewski, H. Speidel, J. Inst. Met. 75 (1948-1949) 417–430.
[30] E. Gebhardt, J. Rexer, Z. Metall. 58 (1967) 616.
[31] E. Rudy, Techn. Rept. AFML–Tr–65-2, 1969, p. 137.
[32] Y.A. Kocherzhinsky, V.Y. Markiv, V.V. Petkov, Russ. Metall. (1973) 134.
[33] N. Dupin, I. Ansara, J. Phase Equilb. 14 (1993) 451–456.
[34] O. Redlich, A.T. Kister, Ind. Eng. Chem. 40 (1948) 345–348.
[35] B. Sundman, B. Jansson, J.O. Andersson, CALPHAD 9 (1985) 153–199.